KRONOS FUSION ENERGY

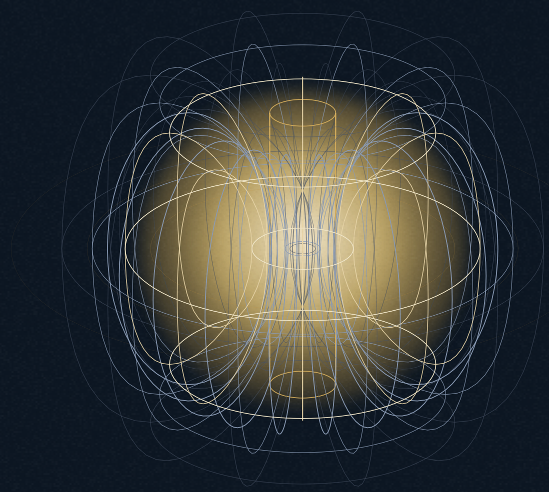

PAPER 2.25 · THE KRONOS 2026 SERIES

# *CAD-Faithful Neutronics for a Compact Spherical-Tokamak Breeder: STEP-to-DAGMC Monte-Carlo Transport Reproducing the 3-D Net Tritium-Breeding Ratio*

Tritium self-sufficiency must survive the geometry a machine is actually built to, not the idealised radial shell that sets the physics target. We transport MeV neutrons directly...

Read it live — 3-D model · physics validator · film series

BY P I FORD AND G L KULCINSKI

2026 · EDITORIAL EDITION

THE OFFICIAL RECORD

# What this document is, and how to read its numbers

This is a combined editorial. It gathers, in one volume, the two design studies Kronos Fusion Energy released in 2026 — a compact spherical-tokamak tritium/helium-3 breeder and a deuterium–helium-3 tandem-mirror generator — together with the intellectual-property estate, the people, and, in the internal edition, the full commercial case. The scientific text is the same text that appears in the arXiv preprints and the journal submissions; the editorial adds the apparatus a reader needs to hold the whole program at once, and nothing in the physics is altered to fit it.

## THE HONESTY STANCE IS THE ASSET

Every headline quantity carries an **evidence class** — DERIVED RECOMPUTED MEASURED REQUIREMENT — and, where a number is a modelled extrapolation rather than a demonstrated value, it is labelled as such and its downside is shown next to it. Several quantities in the underlying corpus moved after first publication; where a value has been withdrawn or restated, the record says so plainly. This is deliberate: a diligence team will find the load-bearing assumptions, so the document surfaces them first.

## TWO EDITIONS

This volume is issued in two editions. The **public edition** (light) carries the physics and the design only — no dollar, price, or per-kilogram figure appears anywhere in it. The **internal edition** (dark) adds the economics, the funding architecture, and the defense-commercial analysis, and is marked *Confidential* accordingly; it is not for public distribution. Where the commercial case rests on a modelled assumption rather than a demonstrated one, it is labelled as such and its downside is shown alongside it, on the same terms as the physics.

| | |
|---|---|
| TITLE | The Kronos Fleet — Hyperion · Aegis · MetroVolt: A Combined Design & Commercialization Study |
| AUTHOR | Priyanca Ford, Founder & CEO, on behalf of Kronos Fusion Energy |
| EDITION | 2026 Combined Editorial · first issue |
| COMPANION WORKS | The five-paper arXiv drop — (1) Breeder, (2) Burner, (3) REBCO magnet & tape, (4) Direct Energy Conversion, (5) AI/ML/Quantum control — with matching numbered Zenodo deposits, plus the IOP journal and IAEA-FEC submissions. Patents were filed before the drop. |
| NAMING | Hyperion = the breeder; Aegis (defense) and MetroVolt (data-center) = one generator in two housings. Internal mode letters (D1, L) do not appear on public surfaces. |
| STATUS | Conceptual design & simulation study. Nothing herein is a construction commitment. |

HOW TO READ THIS VOLUME

# The fleet at a glance, and the way its numbers are marked

This volume opens with *Orientation*, presents the five research papers as a bound sequence, and closes with the *Apparatus*. *Foundations* sets out the three general results both machines rest on. *Paper One* is the Hyperion breeder; *Paper Two* the Aegis / MetroVolt generator; *Papers Three, Four and Five* are the enabling science — high-field REBCO magnets and tape, direct energy conversion, and the AI / ML / quantum control stack. A *Digital Twin & 3-D Model* part follows, then the *Environmental* profile. The *Economics* and levelized cost and the *Business Case* and diligence record appear in the internal edition only; the *Simulations* proof record and the Apparatus — patent portfolio, team, limitations, and sources — close both editions.

## THE FLEET AT A GLANCE

| | HYPERION | AEGIS | METROVOLT |
|---|---|---|---|
| **Role** | Strategic-isotope foundry | Defense installation power | Campus power |
| **Machine** | **Spherical tokamak** | **Tandem mirror** | **Tandem mirror** |
| **Fuel** | Deuterium–tritium | Deuterium–helium-3 | Deuterium–helium-3 |
| **Delivers** | Tritium · $^{3}$He · 14 MeV n | Resilient installation power | Firm campus power |
| **Physics bar** | **Fusion gain only** | Closure (gates named) | Closure + lunar $^{3}$He |
| **In the fleet** | Breeds the fuel | Proves the generator | Commercial destination |

## HOW THE NUMBERS ARE MARKED

Every headline quantity carries an evidence class — DERIVED from first principles, RECOMPUTED from raw data, MEASURED in hardware, or a REQUIREMENT yet to be met. Financial figures carry a case label and are confined to the internal (confidential) edition. Values that moved after first publication are shown as withdrawn or restated rather than quietly changed. A capability you can evaluate is one whose limits are on the page.

## ABSTRACT

# CAD-Faithful Neutronics for a Compact Spherical-Tokamak Breeder: STEP-to-DAGMC Monte-Carlo Transport Reproducing the 3-D Net Tritium-Breeding Ratio

Tritium self-sufficiency must survive the geometry a machine is actually built to, not the idealised radial shell that sets the physics target. We transport 14 MeV neutrons directly on the as-drawn engineering CAD of the Hyperion compact spherical-tokamak breeder (frozen operating point $Q = 3.076$, $P_{\text{fus}} = 85.04$ MW, $I_p = 9.66$ MA, negative triangularity $\delta = -0.30$, $B_0 = 8$ T, elongation $\kappa = 2.0$, major radius $R_0 = 1.20$ m, aspect ratio $A = 2.5$) through a volume-exact STEP → watertight-mesh → DAGMC → OpenMC chain, and confirm a net tritium-breeding ratio (TBR) of **1.120** in the preferred single-null configuration and **1.072** in double-null, both with real ports and divertor penetrations resolved — clearing the 1.05 self-sufficiency gate in full three-dimensional geometry. We state the problem formally: the fixed-source linear Boltzmann transport equation with a 14 MeV plasma emissivity, the breeding ratio as a reaction-rate functional of the angular flux, and the neutron-multiplication balance that beryllium $(n, 2n)$ supplies. We then give the numerical formulation — the watertight-faceting volume identity, the ray-fire streaming query on a bounding-volume hierarchy, the track-length flux estimator, and the batch-means uncertainty that closes as $N^{-1/2}$. The CAD-to-mesh conversion is exact: on a torus-shell verification solid the faceted geometry reproduces the analytic breeder volume to a ratio of 1.000 and returns a per-source-neutron breeding ratio of $1.0145 \pm 0.0039$ with a nuclear heating of 12.63 MeV per source neutron and a 0.31 MB geometry file. The port-free intact torus breeds at 1.262; resolving the penetrations costs 0.142 (single-null) to 0.190 (double-null) in ratio — precisely the first-order correction a one-dimensional model must guess and a CAD-faithful model measures. The single-null budget decomposes into 0.404 inboard and 0.716 outboard, driven by a 0.396-per-source-neutron beryllium multiplication. Against a full ENDF/B-VIII.0 constructive-solid cross-check (1.161/1.118) and the wider breeding ladder (1.15–1.20), the CAD value is the conservative, build-anchored rung. The result removes the coverage-derate caveat from the tritium case and fixes the breeding margin against the fabrication drawing.

Open-access deposit (code & data, CC BY 4.0): DOI 10.5281/zenodo.22645881 · Zenodo community *kronos_fusion_energy*. Explore it live: interactive 3-D model · physics validator.

**Keywords:** neutronics · DAGMC · OpenMC · tritium breeding ratio · CAD-to-mesh · port penetrations · Monte Carlo · spherical-tokamak breeder

CONTENTS

# Table of Contents

NOMENCLATURE

# Symbols, units, and the names of things

| | |
|---|---|
| $Q$ | plasma (fusion) gain, $P_{fus}/P_{aux}$ |
| $Q_E$ | engineering gain, net electric out / recirculating in |
| $H_{98}$ | confinement enhancement over the IPB98(y,2) scaling |
| $Z_{eff}$ | effective ion charge |
| $c_{ee}$ | electron–electron bremsstrahlung leading coefficient, 2.120022 (exact) |
| $\tau_E$ | energy confinement time |
| $I_p$ | plasma current |
| $R_0$, $a$ | major radius, minor radius |
| $\kappa$, $\delta$ | elongation, triangularity |
| $\beta_N$ | normalized plasma beta (Troyon-normalized) |
| *TBR* | tritium breeding ratio |
| *DEC* | direct energy conversion |
| *CF* | plant capacity factor (availability) |
| *FOAK / NOAK / BOAK* | first / $n^{th}$ / best of a kind |
| *Hyperion* | the ST breeder (internal: Mode D2) |
| *Aegis* | the generator, defense/installation housing (internal: Mode M) |
| *MetroVolt* | the generator, data-center housing (Mode M) |

§ 1

# Introduction

## A BLANKET IS DESIGNED TWICE

A breeding blanket is designed twice. It is designed first as a clean one-dimensional radial stack — first wall, multiplier, breeder, reflector, shield — that fixes the physics targets and lets a designer reason about neutron economy analytically. It is built, second, as a fabricated assembly threaded with equatorial ports, gaps between sectors, divertor cassettes and structural penetrations that leak neutrons the one-dimensional model never sees. The distance between the two is exactly where a tritium-self-sufficiency claim is won or lost, and the customary way to bridge it — multiply the one-dimensional breeding ratio by an assumed "coverage factor" — replaces a physics calculation with a guess at the one number that decides whether the fuel cycle closes.

For a compact spherical tokamak (ST) the stakes are sharper still. The ST confines a large plasma current in a small volume behind a slender centrepost [1]; the inboard build is thin, the centrepost — a high-field magnet at a peak of 16.84 T — is a dedicated radiation shield rather than a breeding region [35], and every square metre of outboard blanket must therefore carry a disproportionate share of the breeding load (figure 1). In this geometry a coverage-factor derate is not a small correction bolted onto a comfortable margin — it is a first-order term acting on a margin that is already thin by construction. The honest way to size it is to transport neutrons on the geometry the machine is actually built to.

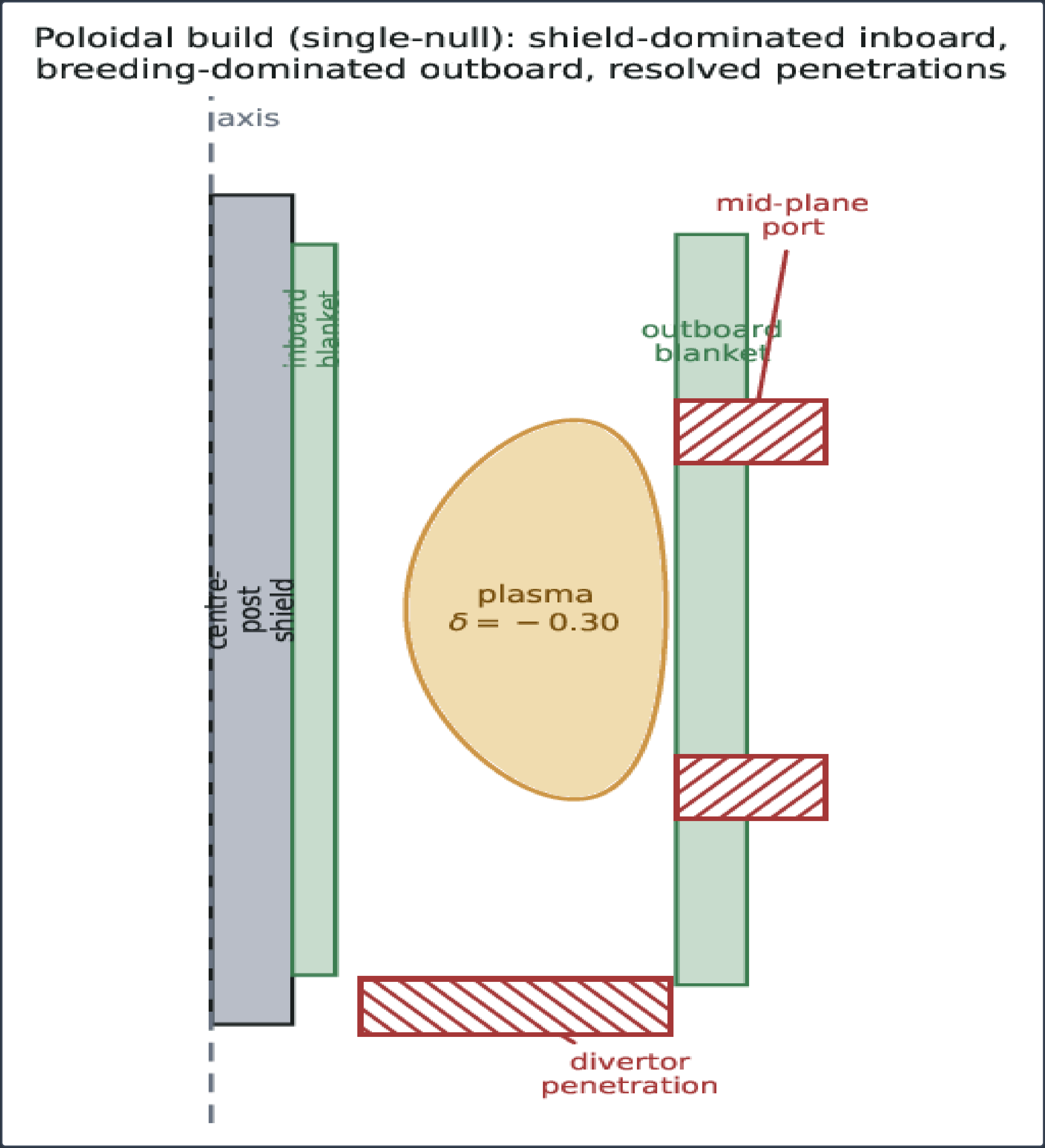


**(Schematic.)** Poloidal build of the single-null configuration. A shield-dominated inboard side (centrepost plus a thin inboard blanket) faces a breeding-dominated outboard blanket around the negative-triangularity ($\delta = -0.30$) plasma; equatorial ports and the divertor penetration (hatched) are the routes through which neutrons leak. No data values are shown; the figure encodes structure only.

## DIRECT-ACCELERATED CAD-BASED MONTE CARLO

The tool that makes this practical is direct-accelerated-geometry Monte Carlo (DAGMC) [2], which lets a continuous-energy transport code track particles on a watertight triangular tessellation of engineering CAD rather than on a hand-built constructive-solid-geometry (CSG) idealisation. Coupled to the open-source Monte-Carlo code OpenMC [3,4], evaluated nuclear data from ENDF/B-VIII.0 [5], and the parametric CAD-to-mesh tooling now standard in the fusion-neutronics community [9,10], the chain has become the reference route for build-fidelity analysis of tokamak blankets, from the fully heterogeneous ITER model [12] to EU-DEMO breeding-blanket studies [13,14,15]. The premise throughout is simple: the geometry the designers ship should be the geometry the neutrons see.

## CONTRIBUTION

This paper reduces that premise to practice on the Hyperion breeder and reports the resulting net TBR. Our contribution is fourfold. *(i)* We give a self-contained formal statement of the neutronics problem (§2): the fixed-source transport equation with a $14$ MeV plasma source, the breeding ratio as a reaction-rate functional, and the multiplication balance. *(ii)* We state the numerical formulation (§3) that makes the CAD-faithful calculation both exact and auditable — the watertight-faceting volume identity, the ray-fire streaming query, the track-length estimator, and the batch-means uncertainty — and prove the conversion volume-exact on a verification solid. *(iii)* We report the net TBR at fabrication fidelity in single-null and double-null configurations with ports and divertor penetrations resolved (§4), decompose it by breeding zone and by neutron economy, and place it on a breeding ladder that runs from the as-drawn recipe to a full-library CSG cross-check. *(iv)* We describe the GPU-HPC campaign that produced the results and makes them reproducible per design revision (§6). Throughout, the design point is the frozen Hyperion operating point and every reported number traces to a Monte-Carlo run in the Kronos Physics De-Risking Register [28] through the serial identifiers cited inline (BR-L2-A22, BV-05B, BR-L2-A7/A7b, P3-NEUT), so each value is auditable.

§ 2

# Governing equations and formal problem

## THE FIXED-SOURCE TRANSPORT EQUATION

Neutrons in the blanket are described by the steady-state, energy- and angle-resolved angular flux $\psi(r, E, \Omega)$, which satisfies the linear Boltzmann transport equation. With macroscopic total cross-section $\Sigma_t$, double-differential scattering kernel $\Sigma_s$, and fixed external source $S$, the transport operator balances streaming, removal and in-scatter:

$$\Omega\cdot\nabla\psi(r, E, \Omega) + \Sigma_t(r, E)\,\psi(r, E, \Omega) = \int_{4\pi}\int_0^\infty \Sigma_s(r, E'\to E, \Omega'\to\Omega)\,\psi(r, E', \Omega')\,\mathrm{d}E'\,\mathrm{d}\Omega' + S(r, E, \Omega).$$

The problem is a fixed-source (non-eigenvalue) one: the blanket is deeply subcritical, and the neutron population is sustained not by fission chains but by the fusion source. Multiplication by $(n, 2n)$ and $(n, 3n)$ reactions is a finite gain on the source, not a self-sustaining chain, and enters equation (1) through the multiplicity in $\Sigma_s$. Boundary conditions are vacuum on the outermost surface (neutrons that cross it are lost) and reflective where symmetry is exploited.

## THE 14 MEV PLASMA SOURCE

The source term factorises into a spatial emissivity, an angular distribution and an energy spectrum,

$$S(r, E, \Omega) = \frac{s(r)}{4\pi}\,\chi(E), \qquad s(r) = \tfrac{1}{2}\,n_D(r)\,n_T(r)\,\langle\sigma v\rangle_{DT}\big(T_i(r)\big),$$

isotropic in the laboratory frame to the accuracy needed here, with $\chi(E)$ the birth spectrum peaked at the $Q$-value $14.06$ MeV of $\mathrm{D(T}, n)^4\mathrm{He}$ and thermally broadened about it. The emissivity is normalised to the frozen fusion power so that the total source rate is set by the operating point,

$$S_n = \int_{V_{\mathrm{pl}}} s(r)\,\mathrm{d}V = \frac{P_{\mathrm{fus}}}{E_{\mathrm{fus}}} = \frac{85.04\ \mathrm{MW}}{17.6\ \mathrm{MeV}} = 3.02\times10^{19}\ \mathrm{n\,s^{-1}},$$

with $E_{\mathrm{fus}} = 17.6$ MeV the total energy released per D–T reaction. Every extensive result below is reported *per source neutron*, so it is independent of this normalisation and depends only on geometry, materials and nuclear data; the normalisation (3) converts a per-source quantity to an absolute rate when required.

## THE BREEDING RATIO AS A FUNCTIONAL OF THE FLUX

Tritium is bred in the lithium-bearing blanket by two channels: the exothermic $^6\mathrm{Li}(n, \alpha)t$ reaction, which dominates at thermal and epithermal energies, and the threshold $^7\mathrm{Li}(n, n'\alpha)t$ reaction, which contributes at fast energies. Writing $N_6, N_7$ for the lithium isotope number densities and $\sigma_{t,6}, \sigma_{t,7}$ for the respective microscopic tritium-production cross-sections, the tritium-breeding ratio is the total tritium production rate per source neutron, a linear functional of the scalar flux $\phi(r, E) = \int_{4\pi}\psi\,\mathrm{d}\Omega$:

$$\Lambda = \frac{1}{S_n}\int_{V_{\mathrm{bl}}}\mathrm{d}V\int_0^\infty \mathrm{d}E\,\Big[N_6(r)\,\sigma_{t,6}(E) + N_7(r)\,\sigma_{t,7}(E)\Big]\,\phi(r, E).$$

Self-sufficiency requires that the machine breed more tritium than it burns, with margin for radioactive decay, extraction and processing inefficiency, in-vessel retention, and a start-up reserve for the next unit. Following the standard fuel-cycle accounting [17,18,19], these losses are folded into a required breeding ratio; for this design the acceptance gate is

$$\Lambda_{\mathrm{net}} \ \geq\ \Lambda_{\mathrm{req}} \approx 1.05,$$

and the object of this paper is to establish where the as-built machine sits relative to (5). The margin budget behind the number $1.05$ is developed in the companion breeding-ladder analysis [33] and the multi-unit fleet accounting [29].

## NEUTRON MULTIPLICATION AND THE ECONOMY BALANCE

Because each source neutron can breed at most one triton before it is absorbed, a bare lithium blanket cannot reach $\Lambda > 1$; a fast-neutron multiplier is required. Beryllium supplies it through $^{9}\mathrm{Be}(n, 2n)2\alpha$, which converts one fast neutron into two above a threshold near $1.85$ MeV. Defining the multiplication as the extra neutrons produced per source neutron,

$$M \;=\; 1 + \frac{1}{S_n}\int_{V_{\mathrm{bl}}} \mathrm{d}V \int_0^{\infty} \mathrm{d}E \; N_{\mathrm{Be}}(r)\,\sigma_{n,2n}(E)\,\phi(r, E) \;+\; \mathcal{O}(\sigma_{n,3n}),$$

the per-source neutron economy closes as a conservation statement between production and loss,

$$\underbrace{M}_{\text{available}} \;=\; \underbrace{\Lambda}_{\substack{\text{consumed by}\\ \text{breeding}}} \;+\; \underbrace{\mathcal{A}_{\mathrm{par}}}_{\substack{\text{parasitic}\\ \text{absorption}}} \;+\; \underbrace{\mathcal{L}}_{\text{leakage}},$$

where $\mathcal{A}_{\mathrm{par}}$ collects captures in structure, coolant and non-breeding materials and $\mathcal{L}$ is the escape through outer surfaces and, decisively for the ST, through ports and penetrations. Equation (7) is the design's lever map: a higher $\Lambda$ is bought by raising $M$ (more multiplier), by lowering $\mathcal{A}_{\mathrm{par}}$ (less parasitic structure) or by lowering $\mathcal{L}$ (more coverage, better penetration shielding). The one-dimensional model can compute $M$, $\Lambda$ and $\mathcal{A}_{\mathrm{par}}$ faithfully but must *assume* $\mathcal{L}$; the CAD-faithful model measures it. The multiplier physics behind $M$ is treated in the beryllium and concept-down-select companions [30,31], and the cross-section uncertainties that dominate the error bar on (4) are ranked in the nuclear-data uncertainty-quantification companion [32].

§ 3

# Numerical formulation and the CAD-to-DAGMC chain

## FROM STEP SOLID TO WATERTIGHT MESH

The pipeline (figure 2) takes a STEP solid exported from the engineering CAD, imprints and merges the surfaces shared between adjacent bodies so that the assembly is topologically consistent, generates a watertight triangular surface mesh, writes a DAGMC `.h5m` geometry backed by the mesh-oriented database MOAB [8], and hands that geometry to OpenMC for continuous-energy transport [2,3]. The parametric construction of the solids and their material tagging follow the community CAD-neutronics tooling [9].

*Watertightness and the manifold condition.* A geometry is transportable only if it is a closed, oriented 2-manifold: every triangle edge is shared by exactly two facets, so that a particle streaming through the mesh always has a well-defined "next" surface and an unambiguous inside/outside. Imprint-and-merge enforces this on shared interfaces; the resulting tessellation $\mathcal{T}_h$ approximates the true boundary $\partial\Omega$ with a chord tolerance $\varepsilon_{\text{chord}} = \max_{x\in\partial\Omega} \operatorname{dist}(x, \mathcal{T}_h)$, the maximum normal deviation of a facet from the surface it represents.

## THE VOLUME IDENTITY AND CONVERSION FIDELITY

The single sharpest test of conversion fidelity is volume conservation, because the breeding functional (4) is an integral over the breeder volume and a systematic volume error propagates directly into $\Lambda$. For a closed triangulation the enclosed volume is given exactly by the divergence theorem applied facet by facet,

$$V_h = \frac{1}{3}\sum_{k\in\mathcal{T}_h} (c_k \cdot \hat{n}_k)\, A_k,$$

with $c_k$ the facet centroid, $\hat{n}_k$ its outward unit normal and $A_k$ its area. For a smooth surface the discretisation error converges quadratically, $|V_h - V(\Omega)| = \mathcal{O}(\varepsilon_{\text{chord}}^2)$, so a sufficiently fine tessellation makes the faceting error negligible against Monte-Carlo noise. On the torus-shell verification solid (serial BR-L2-A22; major radius $180$ cm, inner minor radius $60$ cm, outer $100$ cm, i.e. a $40$ cm breeding shell) the faceted volume reproduces the analytic torus-shell volume to a ratio of

$$V_h/V_{\text{analytic}} = 1.000,$$

confirming that at the tessellation used the mesh conserves the breeder volume to the reported precision (figure 3, table 1). This is the precondition for trusting a CAD-faithful $\Lambda$: if the volume is right, the breeding integral is being taken over the right region.

## PARTICLE TRANSPORT ON THE MESH: THE RAY-FIRE QUERY

Monte-Carlo transport is a sequence of random walks. Each history begins by sampling a source site $(r, E, \Omega)$ from equation (2), then alternates streaming and collision. The streaming step is where DAGMC does its work: the distance to the next material boundary along the flight direction is the smallest positive root of the ray–triangle intersection over the tessellation,

$$d_s(r, \Omega) = \min_{k\in\mathcal{T}_h} \{\, t > 0 : r + t\,\Omega \in \triangle_k \,\},$$

evaluated by the Möller–Trumbore algorithm and accelerated from an $\mathcal{O}(N_{\text{tri}})$ brute-force search to $\mathcal{O}(\log N_{\text{tri}})$ by an oriented-bounding-box hierarchy in MOAB, with signed-distance acceleration for the deepest queries [10]. The collision distance is sampled from the exponential attenuation law, $\ell = -\ln(\xi)/\Sigma_t(E)$ with $\xi \sim \mathcal{U}(0,1)$; if $\ell < d_s$ the neutron collides and its energy and direction are updated from the continuous-energy kernel, otherwise it streams to the surface at $d_s$, crosses into the next cell, and the walk continues until absorption or leakage. Ports and penetrations enter here with no special treatment: they are simply regions the mesh marks as void, through which equation (10) returns a long free path and the neutron streams out — which is exactly the leakage $\mathcal{L}$ that equation (7) requires and the one-dimensional model cannot see.

## TALLY ESTIMATORS AND UNCERTAINTY

Reaction rates are scored with the track-length estimator, which accumulates the product of statistical weight, path length and macroscopic cross-section over every segment a history traverses in a scoring region $V$:

$$\widehat{R}_x(V) = \frac{1}{N}\sum_{i=1}^{N}\sum_{j} w_{ij}\,\ell_{ij}\,\Sigma_x(E_{ij}),$$

so that the breeding ratio (4) is estimated by $\widehat{\Lambda} = \widehat{R}_{t,6} + \widehat{R}_{t,7}$ scored over the blanket and the multiplication (6) by scoring $\Sigma_{n,2n}$. The track-length estimator is preferred over a collision estimator because it accumulates in optically thin void-adjacent regions where collisions are rare — precisely the port neighbourhoods that dominate the leakage correction. Statistical uncertainty is taken from the sample variance of $B$ independent batches of source histories,

$$s_{\Lambda}^2 = \frac{1}{B(B-1)}\sum_{b=1}^{B}\left(\Lambda_b - \overline{\Lambda}\right)^2, \qquad R = \frac{s_\Lambda}{\overline{\Lambda}} \sim \frac{c}{\sqrt{N}},$$

the relative error decaying as $N^{-1/2}$ by the central-limit theorem. Anchored on the verification run ($R = 0.0039/1.0145 = 0.38\%$ at $N = 10^5$), the production configuration ($B = 40$ batches of $2 \times 10^6$ histories, $N = 8 \times 10^7$) reaches a relative error of order $10^{-4}$ on the ratio (figure 4), so the Monte-Carlo noise is far below the port-penalty signal it must resolve.

| QUANTITY | VALUE |
|---|---|
| **faceted volume / analytic volume, eq. (8)** | 1.000 |
| **per-source-neutron breeding ratio** | $1.0145 \pm 0.0039$ |
| **nuclear heating** | 12.63 MeV per source neutron |
| **leakage fraction** | $0.1505 \pm 0.0013$ |
| **DAGMC geometry file size** | 0.31 MB |
| **CAD generation / mesh conversion / transport** | 14.7 / 3.0 / 71.8 s |

CAD-to-DAGMC conversion fidelity on the torus-shell verification solid (serial BR-L2-A22). The faceted mesh conserves the breeder volume exactly and returns physically sensible per-source quantities; timings are for the verification transport of $10^5$ particles.

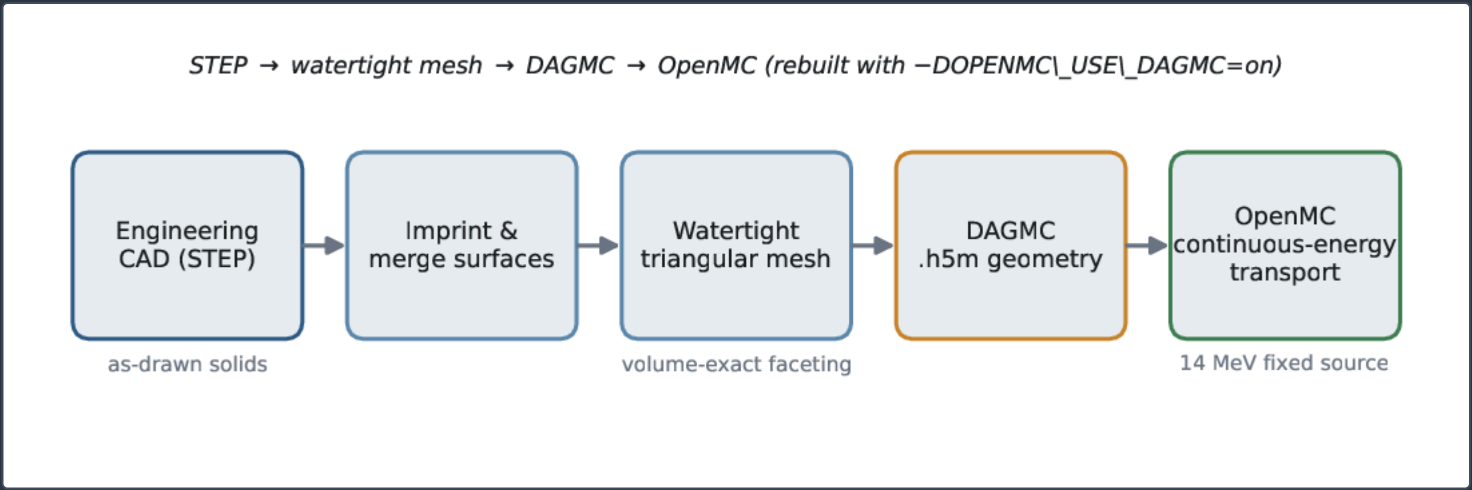


**(Schematic.)** The CAD-faithful transport chain. A STEP solid from the engineering CAD is imprint-and-merged, tessellated into a watertight triangular mesh, written as a DAGMC `.h5m` geometry, and transported in OpenMC rebuilt against the DAGMC backend. The chain is proven end-to-end on the Hyperion geometry (serial BR-L2-A22); no data values are shown.

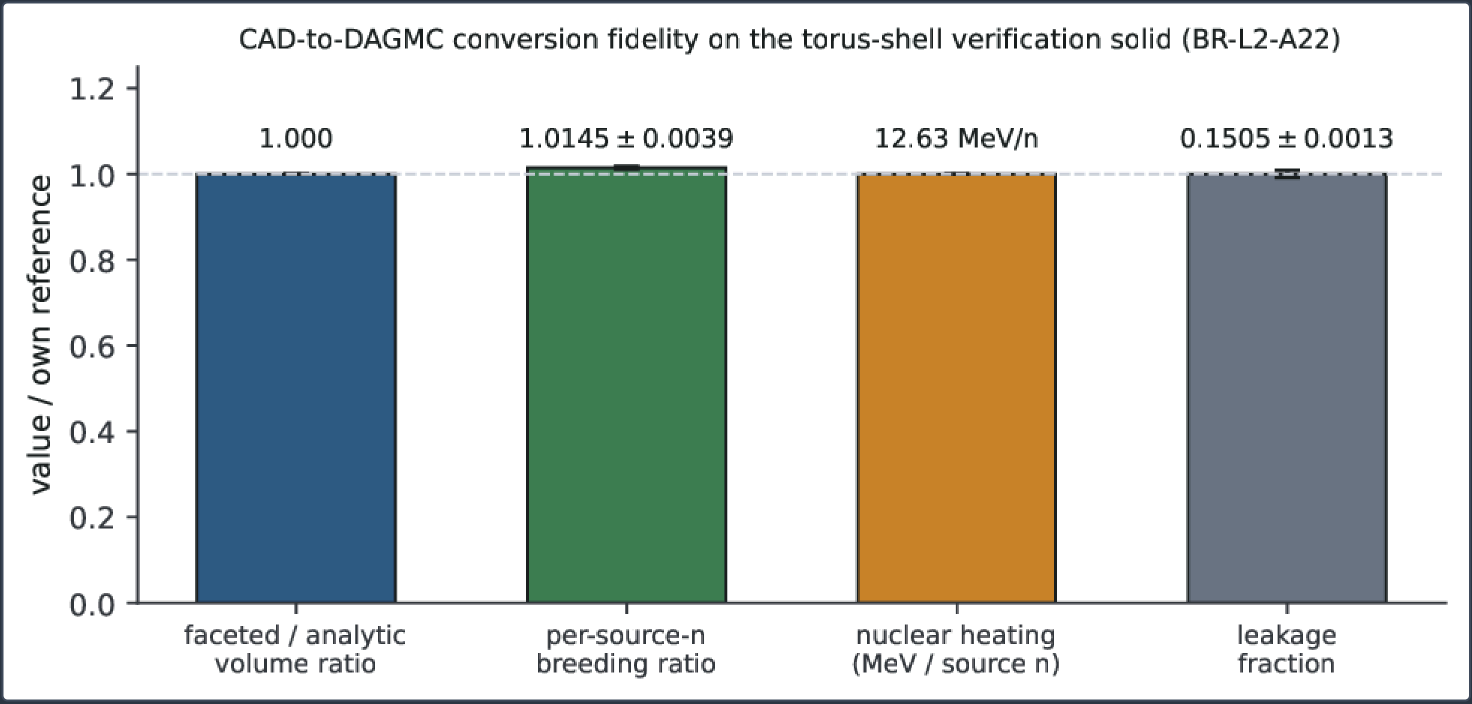


Conversion fidelity on the torus-shell verification solid (BR-L2-A22). The faceted-to-analytic volume ratio is 1.000; the per-source breeding ratio (1.0145 ± 0.0039), nuclear heating (12.63 MeV/n) and leakage fraction (0.1505 ± 0.0013) are physically sensible for a 40 cm lithium shell. Each bar is normalised to its own reference so the four dissimilar quantities share one axis; error bars are the Monte-Carlo $1\sigma$.

## INDEPENDENT-GEOMETRY CROSS-CHECK

Verification is not complete on one geometry engine. Following the verification-first principle of the Kronos campaign, the CAD-faithful result is cross-checked against a fully independent constructive-solid-geometry radial model transported with the same continuous-energy library (serial P3-NEUT; OpenMC with full ENDF/B-VIII.0 [5]). The two engines agree to within the modelling spread, and the honest three-dimensional resolved-port value is carried by the CAD model; the agreement is developed quantitatively in §5. The independent-library cross-check confirms that the reported $\Lambda$ is a property of the geometry and the data, not of any single geometry representation.

§ 4

# Results: net TBR on the as-built geometry

## THE VERIFICATION SOLID FIXES THE PIPELINE

Before the full breeder is transported, the pipeline is fixed on the verification solid. Equation (9) establishes that the conversion is volume-exact; the per-source breeding ratio $1.0145 \pm 0.0039$, the nuclear heating $12.63$ MeV per source neutron, and the leakage fraction $0.1505 \pm 0.0013$ are all physically sensible for a $40$ cm lithium-bearing shell with an open bore (table 1). These verification-solid values are not the breeder canon — the toy shell is not the Hyperion blanket recipe — but they certify that the STEP $\rightarrow$ DAGMC $\rightarrow$ OpenMC chain conserves volume, transports a $14$ MeV source correctly, and closes an energy balance, on a compact $0.31$ MB geometry file and in seconds of wall-clock time (figure 4). With the pipeline fixed, the as-built breeder can be trusted.

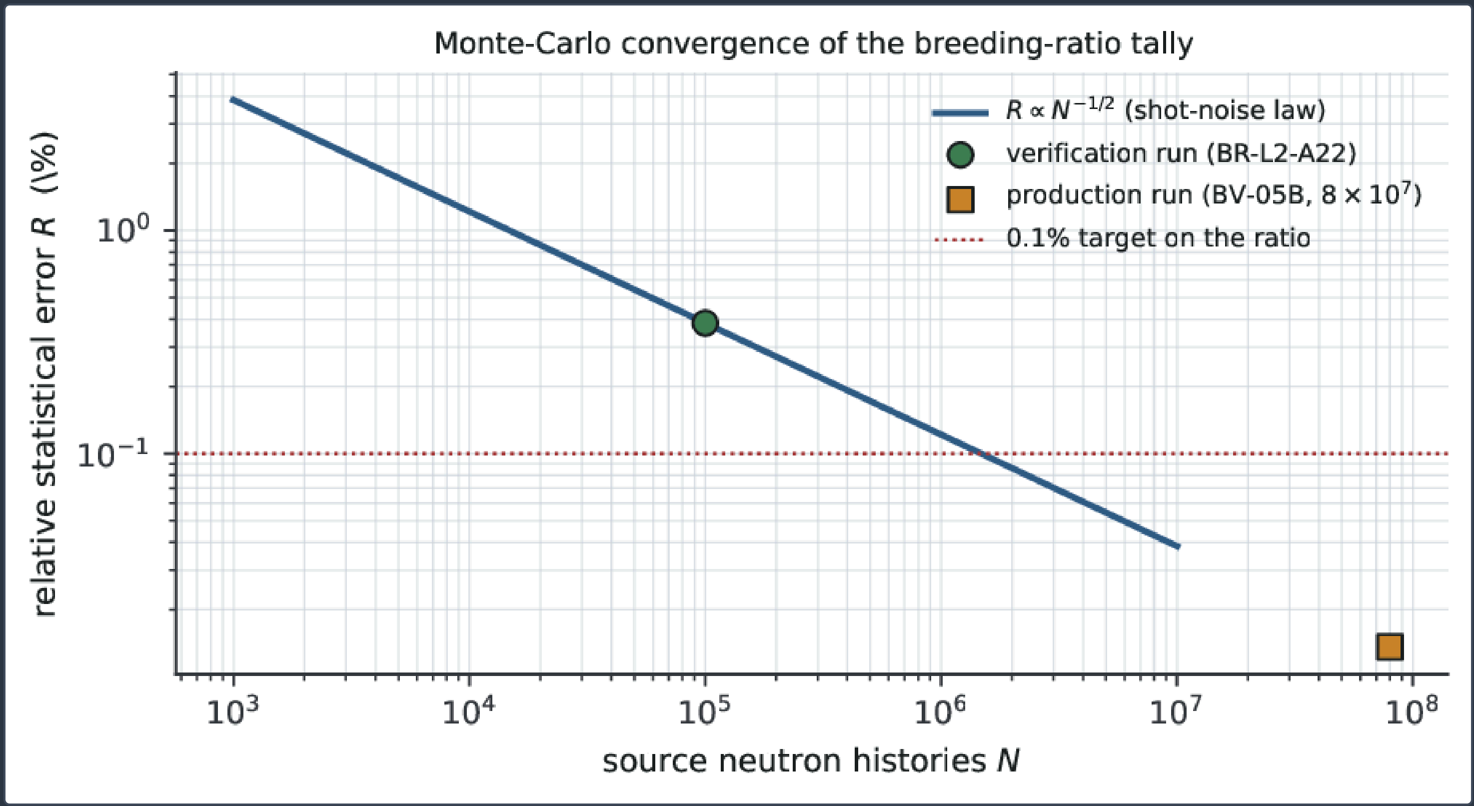


Monte-Carlo convergence of the breeding-ratio tally. The relative statistical error follows the shot-noise law $R \propto N^{-1/2}$ of equation (12), anchored on the verification run ($R = 0.38\%$ at $N = 10^5$, BR-L2-A22). The production configuration ($N = 8 \times 10^7$ histories, BV-05B) reaches a relative error of order $10^{-4}$ on the ratio, well below the $\sim 0.14$ port-penalty signal it must resolve.

## NET TBR IN SINGLE-NULL AND DOUBLE-NULL

The full breeder is transported in two divertor configurations, each with an eight-sector equatorial port pattern and resolved divertor penetrations (serial BV-05B; $B = 40$ batches of $2 \times 10^6$ particles, $^6$Li enrichment 0.90). The results are collected in table 2 and figure 5. Three facts carry the section. First, both fabrication-fidelity configurations clear self-sufficiency: single-null at **1.120** and double-null at **1.072**, each above the 1.05 gate of equation (5) and each with statistical error of order $10^{-4}$ in the ratio. Second, the penalty for building real penetrations is the difference from the port-free intact torus at 1.262: a leakage correction $\mathcal{L}_{\text{port}} = 0.142$ in single-null and 0.190 in double-null. This is a first-order term, and it is precisely the quantity a one-dimensional coverage factor must guess and a CAD-faithful model measures directly through equation (10). Third, single-null is preferred on breeding grounds: it keeps more of the outboard blanket intact and breeds 0.048 higher than double-null, a margin the design banks against the divertor-heat-flux advantage that double-null offers elsewhere in the exhaust trade [31].

| CONFIGURATION | PORTS RESOLVED | NET $\Lambda$ | INBOARD / OUTBOARD | $M-1$ (BE $(n,2n)$) | PORT PENALTY |
|---|---|---|---|---|---|
| **intact torus** | no | 1.262 | — | 0.441 | — |
| **single-null** | yes | **1.120** | 0.404 / 0.716 | 0.396 | 0.142 |
| **double-null** | yes | 1.072 | 0.382 / 0.690 | 0.395 | 0.190 |

Net TBR at fabrication fidelity (serial BV-05B). Both resolved-port configurations clear the **1.05** self-sufficiency gate; single-null is the preferred configuration on breeding grounds. The intact torus is the port-free reference against which the leakage penalty is measured.

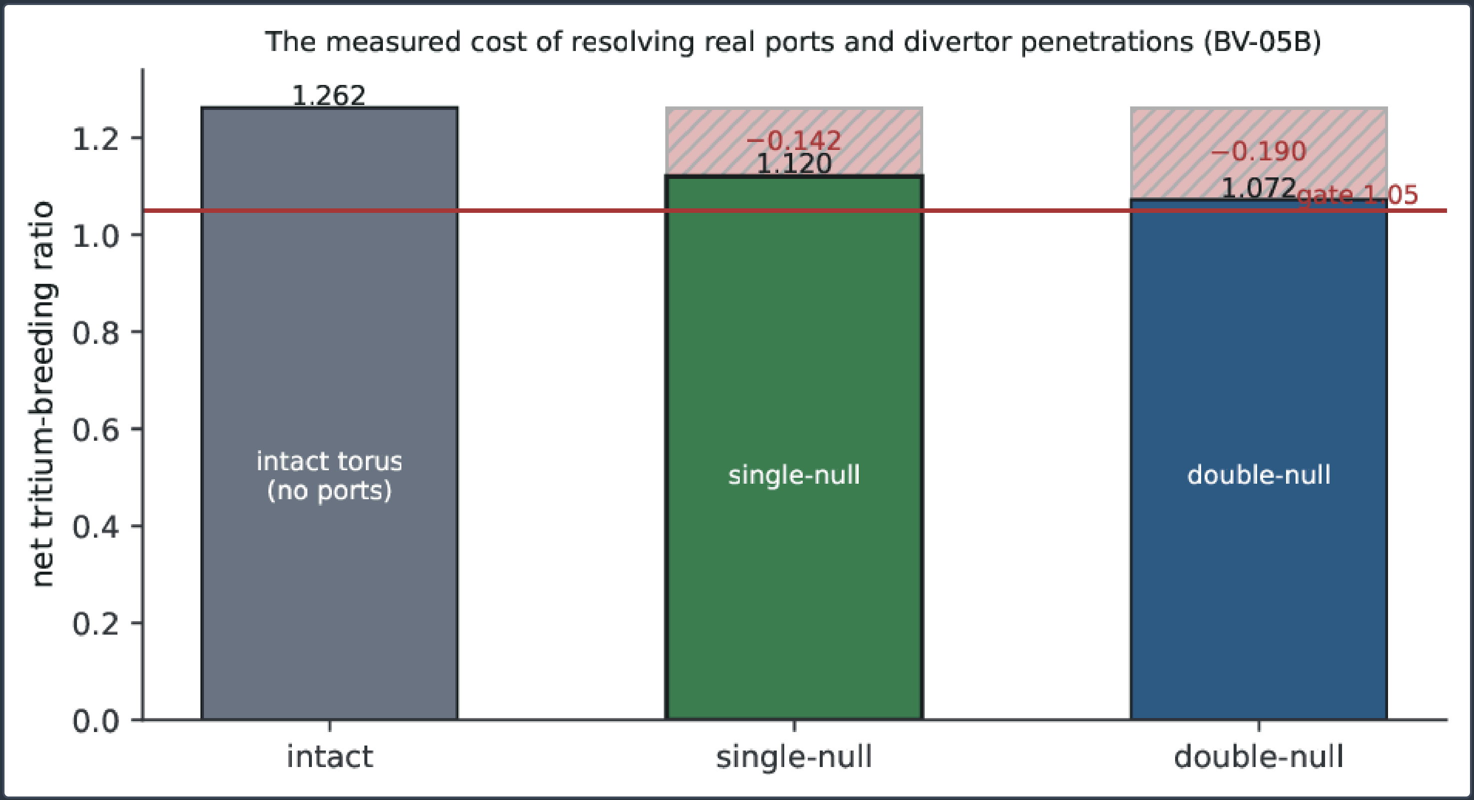


The measured cost of resolving real ports and divertor penetrations (BV-05B). The port-free intact torus breeds at **1.262**; resolving the penetrations lowers the ratio to **1.120** (single-null) and **1.072** (double-null), both above the **1.05** gate. The hatched overlay is the leakage penalty $\mathcal{L}_{\text{port}}$ — the term a one-dimensional model assumes and the CAD model measures.

## WHERE THE TRITIUM IS BRED

The single-null budget decomposes into $0.404$ from the inboard breeder and $0.716$ from the outboard, with a beryllium $(n, 2n)$ multiplication of $M - 1 = 0.396$ neutrons per source neutron supplying the fast-neutron top-up that the $^6\mathrm{Li}(n, \alpha)t$ reaction then converts to tritium (figure 6). The outboard blanket therefore does $716/(404 + 716) \approx 64\%$ of the breeding, consistent with a compact ST in which the thin inboard side is shield-dominated by the centrepost [35]. Double-null shifts the split only slightly ($0.382/0.690$), because its second divertor removes outboard breeding area near the upper X-point. This decomposition is the design's lever map made concrete: outboard coverage and multiplier packing are where breeding margin is bought, exactly as the economy balance (7) predicts.

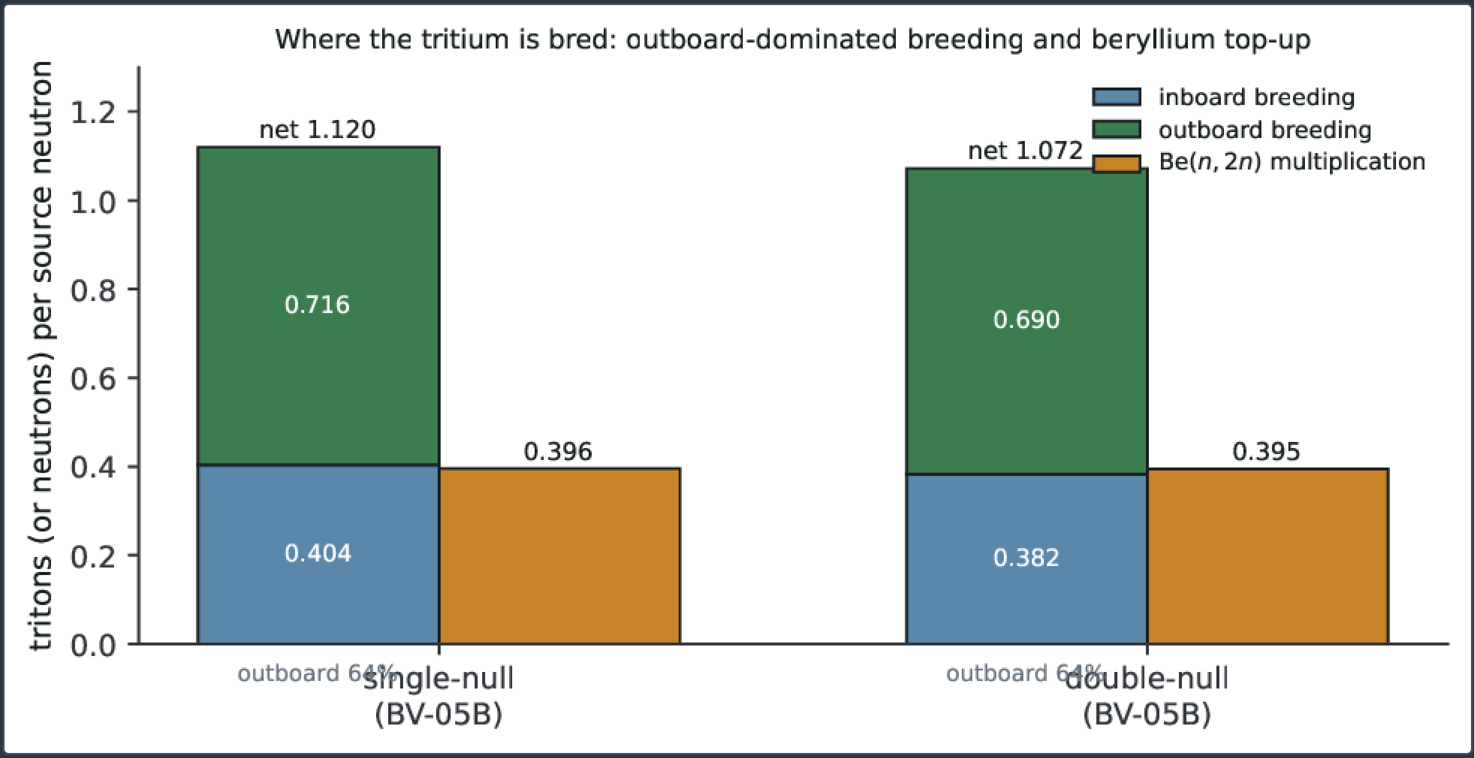


Breeding decomposed by zone (BV-05B). The outboard blanket carries $\approx 64\%$ of the breeding in single-null and $\approx 64\%$ in double-null, as expected for a compact ST with a shield-dominated inboard build; the beryllium $(n, 2n)$ multiplication ($\approx 0.396$ per source neutron) supplies the fast-neutron top-up common to both configurations.

## THE PER-SOURCE NEUTRON ECONOMY

The economy balance (7) closes cleanly on the single-null numbers. Each source neutron is joined by $M - 1 = 0.396$ multiplication neutrons, for $M = 1.396$ available; of these, $\Lambda = 1.120$ are consumed in breeding, leaving $M - \Lambda = 0.276$ to parasitic absorption and leakage combined (figure 7). The multiplier is thus doing exactly the job equation (6) assigns it: without the $0.396$ beryllium top-up the ratio would fall below unity and the fuel cycle would not close, whereas with it the machine breeds a $12\%$ surplus over unity even after the port leakage is paid. That the surplus is modest rather than large is the honest read of the number: the design closes for self-sufficiency but is not sized as a single-unit tritium exporter, a positioning the fleet-export arbiter settles quantitatively [29].

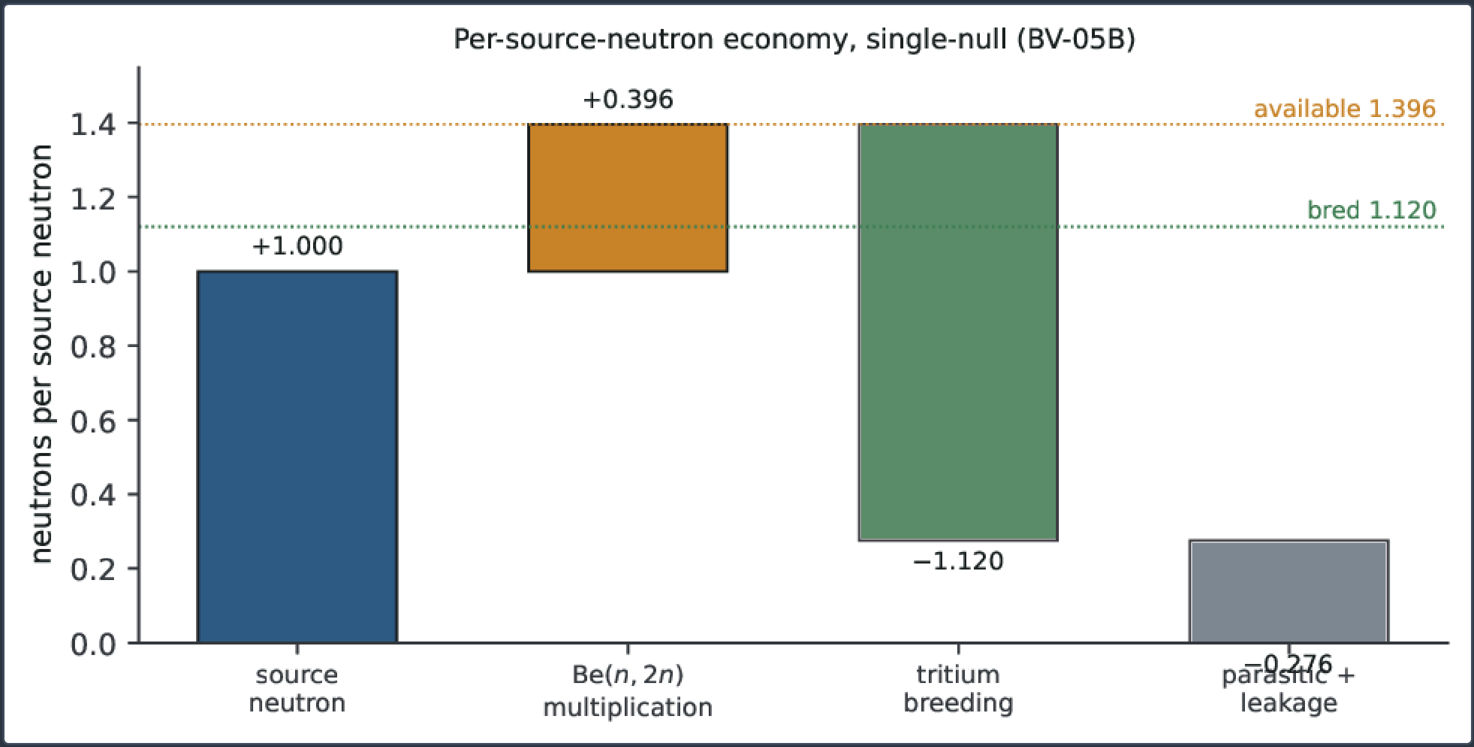


Per-source-neutron economy in single-null (BV-05B), a graphical form of the balance equation (7). One source neutron plus $0.396$ beryllium $(n, 2n)$ neutrons give $1.396$ available; of these $1.120$ are consumed in tritium breeding and $0.276$ go to parasitic absorption and leakage.

§ 5

# The CAD result within the breeding ladder

The CAD-faithful $\Lambda$ is one rung of a consistent breeding ladder that the frozen blanket recipe supports (table 3, figure 8). The literal as-drawn blanket, with beryllium packing in the 9.6–11.8 vol% band, breeds a net 1.026 at the lower packing ($^{6}$Li 0.65) and 1.062 at the upper ($^{6}$Li 0.80) (serial BR-L2-A7); adding a dedicated 5 cm solid-beryllium multiplier layer lifts the same recipe to 1.18–1.20. An independent three-dimensional arbiter places realistic self-sufficiency at 1.15–1.20 (serial BR-L2-A7b), and the full ENDF/B-VIII.0 constructive-solid cross-check returns 1.161/1.118 while confirming that the honest resolved-port value stays at the BV-05B 1.120/1.072 pair (serial P3-NEUT). The rungs agree across a factor that matters: the machine breeds enough tritium for its own fuel cycle across the entire credible modelling spread, and the CAD-faithful 1.120 is the conservative, build-anchored member of that family rather than an outlier. That the constructive-solid model reads slightly higher than the CAD model (1.161 vs 1.120 in single-null) is expected and reassuring: the CSG idealisation cannot leak through ports it does not represent, so it sits above the port-resolved value by roughly the leakage penalty $\mathcal{L}_{\text{port}}$ the CAD model measures.

| BASIS | RECIPE / METHOD | NET $\Lambda$ |
|---|---|---|
| **as-drawn blanket, low Be packing (BR-L2-A7)** | Be 9.6 vol%, $^{6}$Li 0.65 | 1.026 |
| **as-drawn blanket, high Be packing (BR-L2-A7)** | Be 11.8 vol%, $^{6}$Li 0.80 | 1.062 |
| **+ 5 cm solid-Be layer (BR-L2-A7)** | dedicated multiplier | 1.18–1.20 |
| **realistic 3-D arbiter (BR-L2-A7b)** | fleet-set self-sufficiency | 1.15–1.20 |
| **CAD-faithful, resolved ports (BV-05B)** | **single-null / double-null** | **1.120 / 1.072** |
| **ENDF/B-VIII.0 CSG cross-check (P3-NEUT)** | full-library, single-null / double-null | 1.161 / 1.118 |

The breeding ladder — consistent net TBR across modelling fidelity and blanket recipe. The CAD-faithful, resolved-port pair is the conservative, build-anchored rung; every rung clears the 1.05 gate or reaches it by a design lever already in hand.

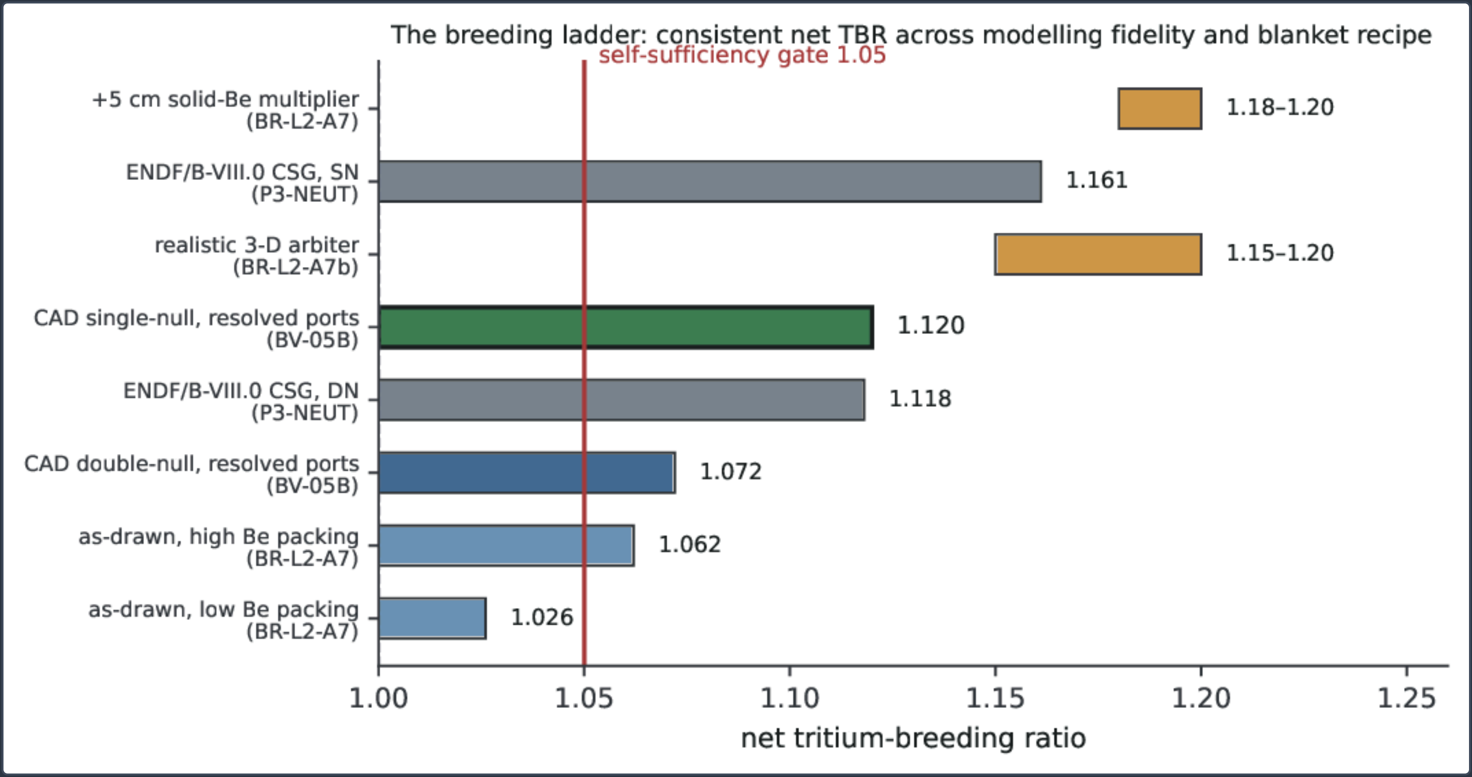


The breeding ladder. Net TBR is consistent across modelling fidelity (as-drawn recipe, CAD-faithful resolved ports, full-library CSG cross-check, realistic arbiter) and blanket recipe. All rungs sit at or above the **1.05** self-sufficiency gate (red); the CAD-faithful single-null value (**1.120**, green) is the conservative, build-anchored member of the family. Ranges are shown as bars.

§ 6

# Computational methodology: the GPU-HPC campaign

Every number in this paper is the output of a Monte-Carlo transport run in the Kronos NVIDIA GPU HPC campaign, and the methodology is reported here so that the results are reproducible per design revision rather than once per program phase.

*Codes run for this paper.* The transport code is OpenMC [3,4], rebuilt from source against the DAGMC backend (configured with –`DOPENMC_USE_DAGMC=on`) so that continuous-energy histories are tracked directly on the watertight CAD tessellation [2]; the mesh geometry is stored and queried through MOAB [8]. The CAD solids are generated and material-tagged with the parametric neutronics tooling of the community CAD-to-mesh chain [9], exported to STEP, imprint-and-merged, and converted to the DAGMC `.h5m` geometry. Nuclear data are the ENDF/B-VIII.0 evaluated library [5], processed to continuous-energy form and Doppler-broadened to the operating temperature; the cross-section channels that dominate the breeding-ratio uncertainty are identified in the nuclear-data uncertainty-quantification companion [32,7]. The independent CSG cross-check (P3-NEUT) runs the same OpenMC binary and the same library on a hand-built radial model, isolating the geometry representation as the only difference.

*Problem scale and acceleration.* The verification transport is $10^5$ source histories; the production configurations are $B = 40$ batches of $2 \times 10^6$ histories each, $N = 8 \times 10^7$ histories per configuration, sufficient to drive the relative error on the breeding ratio to order $10^{-4}$ by equation (12). The calculation is embarrassingly parallel over source histories and over the ensemble of design-revision geometries, which is what the campaign's fleet architecture exploits: the continuous-energy transports are distributed across the NVIDIA GPU HPC campaign nodes (A100/H100/A10 class), while the GPU fabric carries the coupled design-point physics — nonlinear gyrokinetic transport [26], first-principles materials, and the systems-level integration [27] — that fixes the operating point the neutronics is transported at. The full verification transport completes in about ninety seconds of wall-clock time (figure 9; CAD generation 14.7 s, mesh conversion 3.0 s, transport 71.8 s), so the analysis is fast enough to be re-run on every design revision.

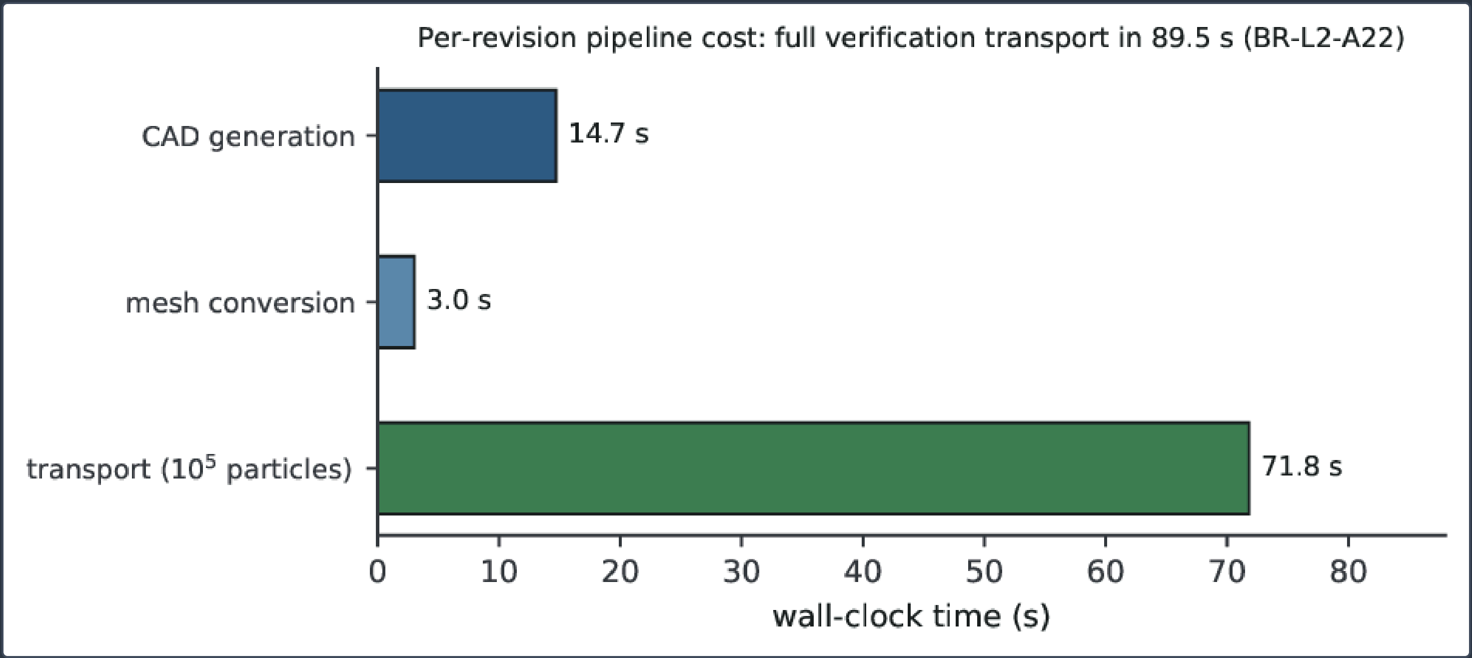


Per-revision pipeline cost (BR-L2-A22). CAD generation, watertight-mesh conversion and a $10^5$-particle verification transport complete in 89.5 s of wall-clock time, so a CAD-faithful breeding check can be run per design revision rather than once per program phase.

*Verification and reproducibility.* The chain is verified at three levels: the volume identity (8) against the analytic solid, the shot-noise convergence (12) against the central-limit law, and the independent-geometry cross-check (CAD vs CSG) against the same nuclear-data library. Each run is seeded deterministically (campaign seed 20260726) and its DAGMC `.h5m` geometry, OpenMC model and tally outputs are archived as frozen anchors in the de-risking register [28], so the byte-identical inputs regenerate the byte-identical results. Two meshing conventions captured during the build — constructing the torus as two 180° half-shells to keep the tessellation watertight, and rebuilding the transport binary against the DAGMC backend — are recorded with the anchor so the pipeline is reproducible by an independent analyst.

§ 7

# Discussion

## THE BREEDING MARGIN STOPS BEING AN ASSUMPTION

The value of transporting neutrons on the CAD is that the breeding margin stops being an assumption. A one-dimensional model must choose a coverage factor to represent ports; that single number multiplies the breeding ratio and therefore decides self-sufficiency by fiat. The CAD model replaces the choice with a measurement: the leakage penalty is $\mathcal{L}_{\text{port}} = 0.142$ in single-null and $0.190$ in double-null (table 2), computed by the ray-fire streaming query (10) on the actual penetrations, and the machine still clears the gate. Because the conversion is volume-exact (equation 9) and the transport is continuous-energy against an evaluated library, the $1.120$ single-null value is anchored to the fabrication drawing with a stated Monte-Carlo uncertainty rather than to an idealised annulus with an assumed derate.

## COMPARISON WITH PUBLISHED CAD-NEUTRONICS PRACTICE

The result sits squarely inside contemporary fusion-neutronics practice. The fully heterogeneous ITER model of Ju\'arez *et al.* [12] established that CAD-faithful transport on the as-built machine can differ materially from idealised models precisely because ports and gaps dominate streaming; EU-DEMO breeding-blanket studies with the HCPB concept report first-wall-integrated TBRs in the $1.1–1.2$ band once penetrations and manifolds are represented [13,14], and DEMO neutronics requirements are routinely stated as a target TBR near $1.05–1.10$ after fuel-cycle losses [15,16]. Our single-null $1.120$ with a measured $0.142$ port penalty is consistent with that literature both in absolute level and in the size of the geometric correction. The value of the present work is not a new absolute number but a build-anchored one: the Hyperion $\Lambda$ is reported on its own CAD, cross-checked against an independent geometry engine and the same ENDF/B-VIII.0 data, and reproducible per revision. The self-sufficiency requirement itself follows the classical fuel-cycle analyses of Abdou and co-workers [17,18,19], whose margin budget is what turns a bare breeding ratio into the $1.05$ acceptance gate used here.

## A LIVING CONSTRAINT ON THE ENGINEERING

Because the full verification transport runs in about ninety seconds, the breeding margin can be tracked as the CAD evolves rather than computed once and trusted. A port relocated for maintenance access, a divertor cassette re-shaped for heat handling, or a manifold re-routed for coolant all change $\mathcal{L}_{\text{port}}$, and each can be priced in TBR before the drawing is frozen. This turns neutronics from a one-time sign-off into a living constraint on the engineering, coupled into the neutronics-and-activation digital twin [36] that shadows the operating point and into the streaming-and-dose analysis [34] that shares the same resolved-penetration geometry.

§ 8

# Limitations

The reported TBR is a beginning-of-life ratio. Lithium-6 burnup over the operating life depletes the breeder and lowers $\Lambda$ with fluence; that time integration is not performed here and is the one open item. It is bounded, not ignored: the enrichment and packing headroom already visible in the breeding ladder (table 3) — the 1.18–1.20 reachable with a dedicated multiplier layer and higher $^{6}$Li enrichment — is the reserve against burnup, and the time-resolved depletion is quantified in the real-time tritium-accountancy twin [37] that carries the in-vessel inventory and self-sufficiency bookkeeping. A second-order caveat is that the reported values are for the frozen blanket recipe; a change of multiplier or breeder chemistry would re-open the ladder, which is the subject of the blanket-and-multiplier concept down-select [31,30].

§ 9

# Conclusion

Transported directly on its as-built CAD through a volume-exact STEP $\to$ DAGMC $\to$ OpenMC chain, the Hyperion compact spherical-tokamak breeder achieves a net tritium-breeding ratio of **1.120** in the preferred single-null configuration and **1.072** in double-null, both with real ports and divertor penetrations resolved and both above the 1.05 self-sufficiency gate. The problem is posed formally — the fixed-source transport equation (1), the breeding functional (4), and the neutron-economy balance (7) — and solved with an auditable numerical formulation whose conversion reproduces the breeder volume exactly (equation 9), whose streaming query resolves the ports the one-dimensional model cannot (equation 10), and whose uncertainty closes as $N^{-1/2}$ (equation 12). The port penalty is measured (0.142/0.190 ) rather than assumed, the breeding decomposes as 0.404 inboard and 0.716 outboard with a 0.396 beryllium multiplication that makes the economy balance close, and the CAD-faithful value sits as the conservative rung of a breeding ladder that agrees from the as-drawn recipe through the full-library cross-check. Tritium self-sufficiency is fixed against the fabrication geometry.

Acknowledgments tocsectionAcknowledgments Part of the Kronos Fusion Energy 2026 design series. The authors thank the Kronos physics de-risking programme for the frozen result set underlying every quantitative claim, and the neutronics-tooling communities behind OpenMC, DAGMC and MOAB whose open codes make CAD-faithful transport possible.

Reproducibility. The CAD-faithful neutronics results are frozen anchors (serials BR-L2-A22, BV-05B, BR-L2-A7/A7b, P3-NEUT) in the Kronos Physics De-Risking Register and are regenerable from the archived DAGMC `.h5m` geometry, OpenMC model and tally outputs under the deterministic campaign seed; transport ran within the NVIDIA GPU HPC campaign. This paper is archived at doi:10.5281/zenodo.22645881; official version: https://www.kronosfusionenergy.com/publications/cad-faithful-neutronics-for-a-compact-spherical-tokamak.html; the register is archived at doi:10.5281/zenodo.22133057.

Data availability tocsectionData availability The DAGMC `.h5m` geometry, the OpenMC model and the tally outputs for the verification solid (BR-L2-A22) and the production configurations (BV-05B), together with the figure-generation script, are archived with the deposit at doi:10.5281/zenodo.22645881, which references the Kronos 2026 series and its de-risking register doi:10.5281/zenodo.22133057. Any economic analysis is reported separately and is not part of the public deposit.

Competing interests tocsectionCompeting interests Provisional patent applications relating to aspects of this work have been filed.

tocsectionReferences

APPARATUS

# *Portfolio, People & Record*

*The intellectual-property estate, the people who built it, the limitations that gate it, and the sources it rests on.*

| | | | |
|---|---|---|---|
| 1 | 4 | 40 | 27 |
| GRANTED PATENT | 2026 PROVISIONALS | TEAM MEMBERS | 2022 PROVISIONALS |

INTELLECTUAL PROPERTY

# The patent portfolio

The estate spans a granted high-field magnet patent, pending utility and 2026 provisional filings that map to the two products, a digital-twin control provisional, a registered trademark application, and the original 2022 provisional family. Every patentable disclosure in the five-paper arXiv drop was protected **before** publication: the breeder and burner provisionals were filed 1–2 August, and a publication-gap omnibus filing the evening before the drop swept up the DEC, plasma-control, and REBCO-winding matter of the three otherwise-unprotected papers. Patent numbers and application serials are matters of public record; claim scope is summarised, not reproduced.

## GRANTED & PENDING UTILITY

| | | |
|---|---|---|
| US 12,009,112 | High-field tilted graded-REBCO magnet architecture (KRONO-002A) · *app. 17/878,550* | GRANTED |
| US 17/878,507 | Core device / method (KRONO-001A) · *utility* | PENDING |

## 2026 PROVISIONAL FILINGS — MAPPED TO THE PRODUCTS

| | | |
|---|---|---|
| 64/124,209 | Hyperion — spherical-tokamak tritium / helium-3 foundry · *breeder · filed Aug 2026* | FILED |
| 64/124,220 | Aegis / MetroVolt — synchrotron-cutoff, fuel-selection & plug-winding · *generator · filed Aug 2026* | FILED |
| 64/115,167 | KRONOS-CTRL digital-twin plant control · *provisional · filed Jul 2026* | FILED |
| 64/005,440 | Integrated spherical-tokamak fusion architecture · *early integrated-architecture filing · filed Mar 2026* | FILED |
| 64/105,530 | Negative-triangularity spherical-tokamak architecture · *foundational ST filing · filed Jul 2026* | FILED |
| 64/128,097 | Publication-gap omnibus — quasineutral two-species expander DEC · provenance-gated / latency-split plasma control · as-built high-field winding & conductor architecture · *filed 7 Aug 2026, the evening before the arXiv drop* | FILED |

## TRADEMARK & ORIGIN

| | | |
|---|---|---|
| FTK-98801894 | Kronos Fusion Energy — trademark application | FILED |
| KR-2022-* | Original provisional family (KR-2022-00001 … 00027) · *27 filings, 2022* | PRIORITY |

The narrow, defensible magnet novelty — the specific conductor and the digital-twin winding optimisation, not high-field REBCO as a category — is the commercial core that can earn ahead of any Q > 1 milestone, with markets in fusion magnet supply, MRI/NMR, accelerators, and proton therapy. The claim is scoped honestly: the high field is a *system field* result, not a stand-alone-coil record; the small-bore plug coil is structurally infeasible as a bare winding but resolved by a stress-managed structural shield (feasible-pending-FEA); and the winding-tape experiment returned a *null result*. The value is the method, not a field record.

THE TEAM

# Founding partners, board, advisors & auditors

Kronos is built by a bench of advanced-fuel-fusion, high-field-magnet, direct-conversion, and materials specialists, with a board and operations team drawn from defense, national laboratories, and industry. Dates are shown as ranges; where a tenure has ended or is term-ending, the range says so.

## FOUNDING PARTNERS — SCIENCE

**Dr. Gerald Kulcinski**
Co-Founder · Helium-3 & Advanced-Fuel Fusion
*UW–Madison · 2023–Present*

**Dr. Carl Weggel**
Chief Scientist / S.M.A.R.T. Design
*MIT Alcator Program · 2022–Present*

**Dr. Robert J. Weggel**
Magnetic Field Design
*MIT Magnet Lab · 2022–Present*

## BOARD

**Priyanca Ford**
Founder & CEO · Executive Board
*2022–Present*

**Bandel Carano**
Finance / Strategy
*Oak Investment Partners / Stanford · 2025–2026*

**Patrick Schweiger**
Fusion Device Engineering
*Oklo / CFS / TerraPower · 2025–Present*

## SCIENTIFIC ADVISORS

**Dr. Steven O. Dean**
Fusion Policy & History
*DOE / Fusion Power Associates · 2025–Present*

**Dr. Patrick H. Diamond**
Plasma Turbulence & Transport
*UC San Diego · 2025–Present*

**Dr. Jack J. Dongarra**
HPC & Numerical Algorithms
*Turing Award · 2025–Present*

**Dr. Nasr M. Ghoniem**
Chief Material Scientist
*UCLA · 2025–Present*

**Dr. Siegfried Glenzer**
Plasma Physics & Laser Fusion
*Stanford / SLAC · 2022–Present*

**Dr. David A. Hammer**
Pulsed-Power Fusion
*Cornell · 2025–Present*

**Dr. Donald A. Spong**
Plasma Theory & Confinement
*ORNL · 2025–Present*

**Dr. Curtis Smith**
Risk Assessment & Nuclear PRA
*MIT / Idaho National Lab · 2025–Present*

**RADM (Ret.) David Goggins**
Naval Engineering & Power-Plant Design
*U.S. Navy · 2023–2026*

**Dr. Konstantin Batygin**
Mathematician
*Caltech · 2022–2025*

**Dr. Ruben Fair**
Magnet Design / ITER Liaison
*PPPL / Jefferson Lab · 2022–2025*

**Dr. Paul S. Weiss**
Materials & Nanotechnology
*UCLA · 2022–2025*

## SCIENTIFIC AUDITORS

**Dr. Wilfred A. Cooper**
Plasma Equilibrium Theory
*EPFL / Swiss Plasma Center · 2025–Present*

**Dr. Ahmed Hassanein**
Plasma–Material Interactions
*Purdue / Argonne · 2025–Present*

**Dr. Patrick E. Hopkins**
Extreme Thermal Materials
*U. of Virginia · 2025–Present*

**Dr. Peter Hosemann**
Materials Joining & Structural Integrity
*UC Berkeley · 2025–Present*

**Dr. Travis W. Knight**
Advanced Nuclear Fuels & Systems
*U. of South Carolina · 2025–Present*

**Dr. Philippe Lebrun**
Cryogenics & Magnet Cooling
*CERN · 2025–Present*

**Dr. Nitendra Singh**
Nuclear Safety & Fuel Cycle
*ITER · 2025–Present*

**Dr. Guido Van Oost**
Magnetic Confinement & Fusion Systems
*Ghent University · 2025–Present*

**Dr. Gary S. Was**
Radiation Materials & Structural Integrity
*U. of Michigan · 2025–Present*

**Dr. Ray Sedwick**
Direct Energy Conversion
*U. of Maryland · 2025*

## OPERATIONS

**Michael Laughlin**
Chief Operating Officer
*2022–Present*

**Martin Owens**
Chief Strategy Officer
*LANL / GE Hitachi · 2022–Present*

**MG (Ret.) Paul Pardew**
Chief Contracting Officer
*Army Contracting Command · 2022–Present*

**David Beck**
Fusion Commercialization
*U.S. Space Force · 2024–Present*

**Sushma Bhatia**
Environmental & Legislative
*Google · 2022–Present*

**Michael De Frenza**
Technology Licensing
*2023–Present*

**MG (Ret.) Robin L. Fontes**
Cybersecurity & Defense
*Army Cyber Command · 2022–Present*

**Vijay Gehani**
Supply Chain & Components
*INOX India · 2024–Present*

**Jon Michel Greenwood**
IT & AI Infrastructure
*Live Nation · 2023–Present*

**Brian C. O'Neill**
National Security
*CIA / ODNI · 2022–Present*

**Gen. (Ret.) Gustave F. Perna**
DoD Liaison
*Operation Warp Speed · 2022–2023*

**Andrea Romero**
Marketing Lead
*2022–Present*

Legal counsel is retained; those roles are held on the internal roster and are not listed here.

SOURCES

# References


1 J E Menard *et al*, Fusion nuclear science facilities and pilot plants based on the spherical tokamak, *Nucl. Fusion* **56** 106023 (2016). doi:10.1088/0029-5515/56/10/106023

2 P P H Wilson, T J Tautges, J A Kraftcheck, B M Smith and D L Henderson, Acceleration techniques for the direct use of CAD-based geometry in fusion neutronics analysis, *Fusion Eng. Des.* **85** 1759 (2010). doi:10.1016/j.fusengdes.2010.05.030

3 P K Romano, N E Horelik, B R Herman, A G Nelson, B Forget and K Smith, OpenMC: a state-of-the-art Monte Carlo code for research and development, *Ann. Nucl. Energy* **82** 90 (2015). doi:10.1016/j.anucene.2014.07.048

4 P K Romano and B Forget, The OpenMC Monte Carlo particle transport code, *Ann. Nucl. Energy* **51** 274 (2013). doi:10.1016/j.anucene.2012.06.040

5 D A Brown, M B Chadwick, R Capote *et al*, ENDF/B-VIII.0: the 8th major release of the nuclear reaction data library with CIELO-project cross sections, new standards and thermal scattering data, *Nucl. Data Sheets* **148** 1 (2018). doi:10.1016/j.nds.2018.02.001

6 M B Chadwick *et al*, ENDF/B-VII.1 nuclear data for science and technology: cross sections, covariances, fission product yields and decay data, *Nucl. Data Sheets* **112** 2887 (2011).

7 A J Koning and D Rochman, Modern nuclear data evaluation with the TALYS code system, *Nucl. Data Sheets* **113** 2841 (2012). doi:10.1016/j.nds.2012.11.002

8 T J Tautges, R Meyers, K Merkley, C Stimpson and C Ernst, MOAB: a mesh-oriented database, Sandia National Laboratories report SAND2004-1592 (2004).

9 J Shimwell *et al*, The Paramak: automated parametric geometry construction for fusion reactor designs, *F1000Research* **10** 27 (2021).

10 P C Shriwise, A Davis, L J Jacobson and P P H Wilson, Particle tracking acceleration via signed distance fields in direct-accelerated geometry Monte Carlo, *Nucl. Eng. Technol.* **49** 1189 (2017).

11 X-5 Monte Carlo Team, MCNP — a general Monte Carlo N-particle transport code, version 5, Los Alamos National Laboratory report LA-UR-03-1987 (2003).

12 R Ju\'arez *et al*, A full and heterogeneous model of the ITER tokamak for comprehensive nuclear analyses, *Nat. Energy* **6** 150 (2021).

13 F A Hern\'andez *et al*, An enhanced, near-term HCPB design as driver blanket for the EU DEMO, *Fusion Eng. Des.* **146** 1186 (2019). doi:10.1016/j.fusengdes.2018.09.014

14 L V Boccaccini *et al*, Objectives and status of EUROfusion DEMO blanket studies, *Fusion Eng. Des.* **109–111** 1199 (2016).

15 U Fischer *et al*, Neutronics requirements for a DEMO fusion power plant, *Fusion Eng. Des.* **98–99** 2134 (2015).

16 G Federici *et al*, Overview of the DEMO staged design approach in Europe, *Nucl. Fusion* **59** 066013 (2019).

17 M A Abdou, E L Vold, C Y Gung, M Z Youssef and K Shin, Deuterium–tritium fuel self-sufficiency in fusion reactors, *Fusion Technol.* **9** 250 (1986).

18 M E Sawan and M A Abdou, Physics and technology conditions for attaining tritium self-sufficiency for the DT fuel cycle, *Fusion Eng. Des.* **81** 1131 (2006).

19 M Abdou, M Riva, A Ying, C Day, A Loarte, L R Baylor, P Humrickhouse, T F Fuerst and S Cho, Physics and technology considerations for the deuterium–tritium fuel cycle and conditions for tritium fuel self sufficiency, *Nucl. Fusion* **61** 013001 (2021).

20 J-Ch Sublet, J W Eastwood, J G Morgan, M R Gilbert, M Fleming and W Arter, FISPACT-II: an advanced simulation system for activation, transmutation and material modelling, *Nucl. Data Sheets* **139** 77 (2017).

21 M R Gilbert, T Eade, C Bachmann, U Fischer and N P Taylor, Activation, decay heat, and waste classification studies of the European DEMO concept, *Nucl. Fusion* **57** 046015 (2017).

22 B N Sorbom *et al*, ARC: a compact, high-field, fusion nuclear science facility and demonstration power plant with demountable magnets, *Fusion Eng. Des.* **100** 378 (2015). doi:10.1016/j.fusengdes.2015.07.008

23 A J Creely *et al*, Overview of the SPARC tokamak, *J. Plasma Phys.* **86** 865860502 (2020). doi:10.1017/S0022377820001257

COLOPHON

# How this document was made

*The Kronos Fleet — Combined Editorial, 2026* is set in **Fraunces** (display), **Gelasio** (text), and **IBM Plex Mono** (data & equations), carried forward from the Kronos editorial design system.

The figures are rendered at 300 dpi from the deposited generator scripts; the document is composed as a single self-contained file with embedded fonts and imagery, paginated to US Letter, and rendered to PDF through a headless Chromium engine in matched light and dark editions.

Every headline quantity carries an evidence class; withdrawn and restated values are marked as such. Nothing herein is frozen beyond the founder-approved Tier-A set.

Explore it live — turn the interactive 3-D model, run the deposited solvers in the physics validator, and watch the companion film series.

LEGAL NOTICE

# Notice, status, and distribution

**Conceptual design & simulation study.** This document reports a conceptual design and simulation study. It is not a construction commitment, a safety-analysis report, a regulatory filing, or an offer of securities. Forward-looking statements — schedules, costs, market sizes, and performance — are estimates subject to the limitations set out in the Simulations part and may change.

**Numbers and their classes.** Quantities are reported with evidence classes and case labels; modelled, assumed, and requirement-class values are identified as such and are not to be quoted without their labels.

**Public edition.** This edition carries the physics and design only; all financial, funding, and defense-commercial content has been removed for public distribution. The scientific text corresponds to the arXiv and journal submissions.

THE 2026 KRONOS SERIES

# One programme, many papers

This editorial is one paper in the Kronos 2026 series — a real fusion company's complete, reproducible physics record for a spherical-tokamak breeder and its low-neutron D–$^3$He tandem-mirror burners. Every headline number is a frozen anchor in the Physics De-Risking Register.

Explore the whole programme: the De-Risking Register, the interactive 3-D model, and the physics validator.

KRONOS FUSION ENERGY

# *CAD-Faithful Neutronics for a Compact Spherical-Tokamak Breeder: STEP-to-DAGMC Monte-Carlo Transport Reproducing the 3-D Net Tritium-Breeding Ratio*

A real fusion company building real machines. Explore the science, live.

Zenodo · doi:10.5281/zenodo.22645881

Read on kronosfusionenergy.com

The Physics De-Risking Register